A Polymer Precursor Route to Metal Borides

Kai Su and Larry G. Sneddon*

Department of Chemistry and the Laboratory for Research on the Structure of Matter, University of Pennsylvania, Philadelphia, Pennsylvania 19104-6323

Received July 9, 1993. Revised Manuscript Received September 9, 1993®

A synthetic route to metal borides that employs processable polymer/metal-oxide precursors is described. The precursor materials are obtained by dispersing metal oxides in the decaborane-dicyanopentane polymer, $(-B_{10}H_{12}NC-(CH_2)_5-CN-)_x$. Subsequent pyrolyses of the dispersions above 1400 °C afford metal borides, including TiB_2, ZrB_2, HfB_2, NbB_2, and TaB_2 in high chemical and ceramic yields. The metal boride powders were found to be highly crystalline with grain sizes dependent on processing temperatures. The ceramic conversion reactions are proposed to involve *in situ* generation of amphorous BCN materials, followed by solid-state reduction of the metal oxides to produce the final boride products. Precursor dispersions formed from submicron metal oxides, along with a suitable surfactant, can be used to generate an emulsion from which metal boride coatings on graphite plates can be obtained.

Introduction

Metal borides are, in general, chemically inert, high melting, and extremely hard solids with high degrees of thermal and electronic conductivities. They are important high heat- and wear-resistant engineering ceramics which may be used in various hostile environments.[1] Conventional methods for the syntheses of metal borides are based on the high-temperature carbothermal/borothermal reduction of metal oxides with a boron–carbon source, such as boron oxide/carbon or boron carbide.[1a,e] The syntheses of submicron metal boride powders or metal boride films from a number of organometallic precursors have also been achieved.[2-4] We reported in an earlier communication[5] that TiB_2 and ZrB_2 powders can be synthesized in high yields by means of a potentially general polymer–precursor route employing dispersions of metal oxides in decaborane–dicyanopentane polymers. Seyferth has also recently communicated[6] the use of a similar method, in which metal powders dispersed in decaborane–diamine polymers are the precursors, to achieve metal boride materials. We report in this paper full details of our work and the extension of this method to produce other metal borides, including HfB_2, TaB_2, and NbB_2.

Experimental Section

Materials. The HfO_2, Nb_2O_5, and Ta_2O_5 were purchased from Aldrich and ground with a mortar and pestle. Submicron TiO_2 and ZrO_2 and a block copolymer surfactant (du Pont AB dispersant, 55 wt % in toluene) samples were obtained from Dr. Michael Fryd at the du Pont Marshall Laboratory and used as received. Decaborane(14) was obtained from Callery Chemical Co. Graphite plates were sliced from graphite rods (POCO DFP-1). The surfaces of the substrates were first smoothed with sand paper, then polished with 1-μm alumina. The plates were cleaned with ultrasonic agitation in an acetone bath and dried in vacuo for 1 h at room temperature before use. Anhydrous THF was obtained from Aldrich (H_2O < 0.003 ppm) and used as received. The argon (grade 5) was purchased from Airco and further purified by passing through an oxygen scavenger (Lab Clear, O_2 < 1 ppm) that was installed between the gas tank and the tube furnace.

Instrumentation. All pyrolyses under 1900 °C were performed in a Linberg tube furnace under an argon atmosphere. The pyrolyses at or above 1900 °C were achieved in the graphite furnace of an Astro Industry hot press, Model 1000-3070 HP under vacuum. The temperature was measured with a L & N optical pyrometer. X-ray powder diffraction (XRD) spectra were recorded on a Rigaku Geigerflex X-ray diffractometer using Cu Kα radiation. The XRD peaks of the metal oxides, metal borides, B_4C, graphite, BN, and B_2O_3 were indexed according to the JCPDS diffraction data file (1988). Scanning electron microscopy (SEM) and transmission electron microscopy (TEM) were carried out on a Philips 500X scanning electron microscope and a Philips 400X transmission electron microscope, respectively. Thermogravimetric analyses (TGA) were performed on a Seiko TG/DTA 320 attached to a Fison Instruments Thermolab mass spectrometer. Auger electron spectra (AES) were obtained on a Perkin-Elmer Phi 600 scanning Auger microprobe. Ar^+ ion sputtering was performed using a differentially pumped ion gun and the ion sputtering rate was 125 Å/min as measured on a 1000-Å film of

• Abstract published in *Advance ACS Abstracts,* October 15, 1993.

(1) For general reviews of the syntheses, structure and properties of metal borides see: (a) Greenwood, N. N.; Parish, R. V.; Thornton, P. *Q. Rev.* **1966**, *20*, 441–464. (b) Matkovich, V. I. *Boron and Refractory Borides*; Springer-Verlag: New York, 1977. (c) Post, B. In *Boron, Metallo-Boron Compounds and Boranes*; Adams, R. M., Ed.; Interscience: New York, 1964; pp 301–372. (d) Greenwood, N. N. *The Chemistry of Boron*; Pergamon: New York, 1975; pp 697–731. (e) Thompson, R. In *Progress in Boron Chemistry*; Pergamon: New York, 1970; Vol. 2, pp 173–230. (f) Hoard, J. L.; Hughes, R. E. In *The Chemistry of Boron and Its Compounds*; Muetterties, E. L., Ed.; Wiley: New York, 1967; pp 25–154.

(2) For example: (a) Gallagher, M. K.; Rhine, W. E.; Bowen, H. K. In *Ultra-Structure Processing of Advanced Ceramics*; Mackenzie, J. D., Ulrich, D. R., Eds.; Wiley: New, York, 1988; p 901. (b) Brynestad, J.; Bamberger, C. E.; Heatherly, D. E.; Land, J. F. *High Temp. Sci.* **1985**, *19*, 41–49. (c) Low, I. M.; McPherson, R. *J. Mater. Sci. Lett.* **1989**, *8*, 1281–1283. (d) Rice, G. W.; Woodin, R. L. *J. Am. Ceram. Soc.* **1988**, *71*, C181–C183.

(3) For examples see: (a) Jensen, J. A.; Gozum, J. E.; Pollina, D. M.; Girolami, G. S. *J. Am. Chem. Soc.* **1988**, *110*, 1643. (b) Wayda, A. L.; Schneemeyer, L. F.; Opila, R. L. *Appl. Phys. Lett.* **1988**, *53*, 361–363. (c) Pierson, H. O.; Randich, E.; Mattox, D. M. *J. Less-Common Met.* **1979**, *67*, 381–388. (d) Takahashi, T.; Itoh, H. *J. Cryst. Growth* **1980**, *49*, 445–450.

(4) (a) Shikama, T.; Sakai, Y.; Fukutomi, M.; Okada, M. *Thin Solid Films* **1988**, *156*, 287. (b) Prater, J. T. *Surf. Coat. Technol.* **1986**, *29*, 241. (c) Karner, H.; Laimer, J.; Stori, H. *Surf. Coat. Technol.* **1989**, *39*, 293–300.

(5) Su, K.; Sneddon, L. G. *Chem. Mater.* **1991**, *3*, 10–12.

(6) Seyferth, D.; Bryson, N.; Workman, D. P.; Sobon, C. A. *J. Am. Ceram. Soc.* **1991**, *74*, 2687–2689.

0897-4756/93/2805-1659$04.00/0

Table I. Polymer Pyrolysis Results

polymer	ceramic	temp (°C)/ time (h)	char yield (%)	compositions
1.04 g	0.81 g	1250/1.0	77.9	$N_{1.00}C_{2.70}B_{5.24}$
0.50	0.32	1450/12.0	64.0	$N_{1.00}C_{2.08}B_{4.19}$
1.03	0.50	1900/25.0	48.5	$N_{1.00}C_{14.29}B_{17.14}$

Table II. Summary of Metal Oxide/Polymer Dispersion Preparations

metal oxide	metal oxide wt (g)	polymer wt (g)	M:B:C ratio
TiO_2	5.00	3.89	1.0:2.4:1.7
ZrO_2	5.00	2.52	1.0:2.4:1.8
HfO_2	2.50	0.73	1.0:2.4:1.8
Nb_2O_5	2.00	1.06	1.0:2.7:2.1
Ta_2O_5	3.00	0.96	1.0:2.5:1.9

silicon dioxide on silicon. It was assumed that the sputtering rate of TiB_2 was similar. Elemental analyses of the metal borides were performed at Pascher, Remagen, Germany. The remaining analyses were performed at Gailbraith Laboratories, Knoxville, TN.

Synthesis of Decaborane–Dicyanopentane Polymer. Decaborane–dicyanopentane polymer was prepared according to the literature method.[7] A 3.47-g (28.4 mmol) sample of $B_{10}H_{14}$ was dissolved in 3.49 g (28.6 mmol) of 1,5-dicyanopentane in a 250-mL two-neck flask fitted with a septum and a condenser. The mixture was then heated in an oil bath at 80 °C for 15 h under argon. Hydrogen evolution was observed and the liquid became more and more viscous until 6.8 g (98% conversion) of a golden solid was obtained. At the end of the reaction, ~0.04 g of $B_{10}H_{14}$ was recovered on the condenser. The polymer was used without further purification. For $(-B_{10}H_{12}NC(CH_2)_5CN-)_x$: Anal. Calcd: C, 34.70%; B, 44.65%; N, 11.57%; H, 9.09%. Anal. Found: C, 34.84%; B, 41.78%; N, 11.93%; H, 9.09%. IR (KBr, cm^{-1}) 2936 (s), 2908 (s), 2865 (m), 2510 (vs), 2326 (m), 2241 (w), 1893 (m), 1514 (m), 1457 (s), 1407 (s), 1350 (m), 1329 (m), 1124 (m), 1074 (m), 996 (s), 974 (s), 939 (s), 861 (w), 790 (s), 737 (s), 677 (m), 649 (m), 521 (w), 482 (w).

Polymer Ceramic Conversions. A polymer sample was weighed in a graphite crucible under argon. The crucible was then placed in a mullite tube that was immediately transferred to a tube furnace. After an argon purge for 5 min, the sample was heated to the desired temperature at 10 °C/min. Upon cooling to room temperature, black materials were obtained. Anal. Found: (1250 °C) C, 30.45%; B, 53.38%; N, 13.26%; H, <0.05%; (1450 °C) C, 29.35%; B, 53.26%; N, 16.60%; H, <0.05%.

In another experiment, a graphite crucible containing the polymer sample was transferred into the Astro furnace. After the furnace was evacuated to 5×10^{-6} Torr, the oven was heated to 1900 °C over a ~6-h period, held at this temperature for 25 h, then cooled to room temperature. Anal. Found (1900 °C) C, 46.09%; B, 50.40%; N, 3.56%; H, <0.05%.

The polymer pyrolysis conditions and the ceramic compositions for all reactions are given in Table I.

Preparation of Metal Oxide/Polymer Dispersions. In a typical process, summarized in Table II, a sample of metal oxide powder was added to a THF solution of the polymer and the mixture stirred vigorously with a magnetic stirbar for ~15 min. The solvent was then vacuum evaporated while maintaining ultrasonic agitation. The resulting yellow solid was dried in vacuo for 1 h and stored under argon until pyrolysis.

Synthesis of Metal Borides. A sample of the metal oxide/polymer dispersion was weighed in a graphite crucible under argon. For pyrolyses <1900 °C, the crucible was then placed in a mullite tube that was immediately transferred to a tube furnace. After an argon purge for 5 min, the sample was heated at 10 °C/min to the desired temperature under a continuous flow of argon. The sample was then cooled to room temperature.

For pyrolyses ≥1900 °C, the graphite crucible containing a sample of a precursor material was placed in the Astro graphite furnace and evacuated to 5×10^{-6} Torr. The furnace temperature was then brought to either 1900 or 2000 °C over a ~5–6-h period and held at that temperature for 2 or 3 h, before cooling to room temperature. The pyrolysis conditions and compositions of the resulting dark grey metal boride powders are presented in Table III. TiB_2: Anal. Calcd: Ti, 68.9%; B, 31.1%. Found: (1450 °C) Ti, 68.9%; B, 29.9%; N, <0.2%; C, 0.14%; O, 1.4%; H, <0.05%; (2000 °C) Ti 68.3%; B, 30.4%; N, 0.35%; C, 0.16%; O, 0.3%. ZrB_2: Anal. Calcd: Zr, 78.8%; B, 19.2%. Found: (1450 °C) Zr, 77.1%; B, 16.1%; N, 1.70%; C, 0.14%; O, 4.97%; H, <0.1%; (1650 °C) Zr, 78.3%; B, 18.5%; N, <0.1%; C, <0.03%; O, 1.53%; (2000 °C) Zr, 80.3%; B, 19.2%; N, <0.1%; C, 0.14%; O, 0.2%. HfB_2: Anal. Calcd: Hf, 89.2%; B, 10.8%. Found: (1900 °C) Hf, 88.9%; B, 10.0%; N, 0.01%; C, 0.8%; O, 0.3%; H, <0.1%. NbB_2: Anal. Calcd: Nb, 81.1%; B, 18.9%. Found: (1480 °C) Nb, 73.8%; B, 19.1%; N, 2.9%; C, 0.2%; O, 3.8%; H, <0.1%. (1900 °C) Nb, 81.1%; B, 13.8%; N, <0.2%; C, 2.6%; O, 0.2%; H, 0.02%. TaB_2: Anal. Calcd: Ta, 89.3%; B, 10.7%. Found: (1480 °C) Ta, 85.3%; B, 11.8%; N, 2.0%; C, <0.1%; O, 1.3%; H, <0.1%; (1900 °C) Ta, 84.8%; B, 9.02%; N, <0.2%; C, <0.8%; O, 1.53%; H, 0.03%.

Table III. Pyrolysis Results

metal oxide	dispersion (g)/ prod yield (g)	temp (°C)/ time (h)	theor/ obs ceram yield (%)	chem yield (%)[a]	product composition
TiO_2	0.21/0.18	580/2	48.9/85.7		
TiO_2	0.37/0.32	1000/2	48.9/86.5		
TiO_2	0.21/0.17	1100/2	48.9/81.0		
TiO_2	0.98/0.57	1300/2	48.9/58.2		
TiO_2	0.34/0.17	1450/1	48.9/50.0		
TiO_2	0.87/0.41	1450/21	48.9/47.1	96.3	$Ti_{1.00}B_{1.92}O_{0.06}$
TiO_2	3.8/1.67	2000/3	48.9/43.9	89.8	$Ti_{1.00}B_{1.97}O_{0.01}$
ZrO_2	0.26/0.23	1000/2	61.1/88.5		
ZrO_2	0.71/0.48	1300/2	61.1/67.6		
ZrO_2	0.26/0.16	1450/1	61.1/61.5		
ZrO_2	0.93/0.50	1450/21	61.1/53.76	88.3	$Zr_{1.00}B_{1.76}O_{0.37}N_{0.14}$
ZrO_2	0.90/0.53	1650/7	61.1/58.9	96.4	$Zr_{1.00}B_{1.94}O_{0.11}$
ZrO_2	0.96/0.54	2000/3	61.1/56.0	92.4	$Zr_{1.00}B_{2.02}$
HfO_2	0.80/0.61	1450/21	73.4/76.3		
HfO_2	1.08/0.75	1900/4	73.4/69.4	94.7	$Hf_{1.00}B_{1.86}O_{0.04}N_{0.13}$
Nb_2O_5	0.22/0.20	580/2.5	56.3/90.9		
Nb_2O_5	0.40/0.34	1100/2.5	56.3/85.0		
Nb_2O_5	0.33/0.24	1200/2.5	56.3/72.7		
Nb_2O_5	0.24/0.16	1300/2.5	56.3/66.7		
Nb_2O_5	1.30/0.73	1480/12	56.3/56.2	99.7	$Nb_{1.00}B_{2.22}O_{0.30}N_{0.26}$
Nb_2O_5	1.46/0.77	1900/4	56.3/52.7	93.6	$Nb_{1.00}B_{1.46}O_{0.25}$
Ta_2O_5	0.27/0.25	580/2.5	70.0/92.6		
Ta_2O_5	0.41/0.38	1100/2.5	70.0/92.7		
Ta_2O_5	0.44/0.35	1200/2.5	70.0/79.5		
Ta_2O_5	0.31/0.23	1300/2.5	70.0/74.2		
Ta_2O_5	1.52/1.06	1480/12	70.0/69.7	99.6	$Ta_{1.00}B_{2.32}O_{0.17}$
Ta_2O_5	1.64/1.02	1900/4	70.0/62.2	89.5	$Ta_{1.00}B_{1.78}O_{0.20}$

[a] Chemical yield of the boride refers to the mole percent of the starting metal (in the initial metal oxide) that was converted to metal boride.

TiB_2 Coatings on Graphite Plates. In a typical experiment, a 0.15-g sample of submicron TiO_2 was added to ~5 mL of THF containing 0.12 g of the polymer and 0.15 g of the dispersant solution. The precursor material was thoroughly mixed by ultrasonic agitation for 15 min. The THF was then vacuum evaporated until ~2.5 mL of solution remained. Coatings were then achieved by either dipping the substrate into this viscous emulsion or by spreading the emulsion on the substrate under an argon atmosphere. The coated graphite plates were then transferred to a graphite boat and heated to 1450 °C (2 °C/min) and held at that temperature for 2 h in a tube furnace. After cooling to room temperature, several samples were reheated at 2000 °C in vacuo for 2 h in a manner similar to that described above.

Pyrolysis of du Pont AB Dispersant. A 0.64-g sample of the du Pont AB dispersant was placed in a graphite crucible that was transferred to a tube furnace. After an argon purge for 5 min, the sample was heated at 10 °C/min to 1150 °C under a

(7) Green, J.; Fein, M. M.; Mayes, N.; Donovan, G.; Israel, M.; Cohen, M. S. *Polym. Lett.* **1964**, *2*, 987–989.

continuous flow of argon. Subsequent cooling of the sample to room temperature resulted in only a trace of black residue.

A TGA analysis of the thermal decomposition of du Pont AB dispersant showed two major weight losses. After the initial 9% weight loss from 140–290 °C, the organic polymer decomposed quickly in the 300–450 °C range with less than 1% char left at 850 °C.

Results and Discussion

Metal borides have classically been synthesized by a number of high-temperature techniques, with one of the most common being the carbothermal reduction of metal oxides with boron carbide and carbon.[1,8,9] This method has been successfully applied to the large-scale preparation of, for example, selected metal hexaborides and tetraborides and to the diborides of most transition metals:

$$MO_2 + {}^1/_2B_4C + {}^3/_2C \rightarrow MB_2 + 2CO \quad (1)$$

Although efficient, the carbothermal reduction can be used to generate metal borides only in powder form, since neither metal oxides nor boron carbide are processable. In addition, the final products are usually contaminated with carbon and oxygen.[10] The recent development of several polymeric precursors[11] to boron carbide suggested to us that a processable metal boride precursor might be obtained by dispersing a metal source, such as a metal oxide, in a boron carbide polymeric precursor. Subsequent heating could then result in either *in situ* generation of a boron–carbon material followed by reduction to produce the boride, or direct reaction of the polymer with the metal oxide to give the final boride product:

$$MO_2 \text{ or } M_2O_5 + \text{polymer} \rightarrow B_4C + C + MO_2 \text{ or } M_2O_5 \rightarrow MB_2 + CO \quad (2)$$

The key requirements for the polymer component of the metal oxide/polymer dispersions are that it is stable, soluble and contain the approximate boron to carbon ratio needed for the formation of the boride and removal of oxygen. In addition, the polymer must be readily synthesized and have high ceramic yields at reasonably low temperatures. One series of polymers that satisfy these criteria is the decaborane–dinitrile polymers, which can be prepared in high yields from the condensation polymerization of decaborane with dinitriles.[7] Because of its good solubility in ethers and its relatively high B:C ratio, the decaborane–dicyanopentane polymer was chosen for this study:

$$B_{10}H_{14} + NC(CH_2)_5CN \xrightarrow{\Delta} (-B_{10}H_{12}N{\equiv}C(CH_2)_5C{\equiv}N-)_n + H_2 \quad (3)$$

The polymer synthesis[7] was carried out by heating a solution of an equivalent amount of decaborane dissolved in 1,5-dicyanopentane at 80 °C for 15 h. The polymer was obtained as a slightly air-sensitive golden solid in almost quantitative yield. Elemental analysis showed a 1:1 decaborane to dicyanopentane ratio. The polymer is readily soluble in ethers but decomposes before melting.

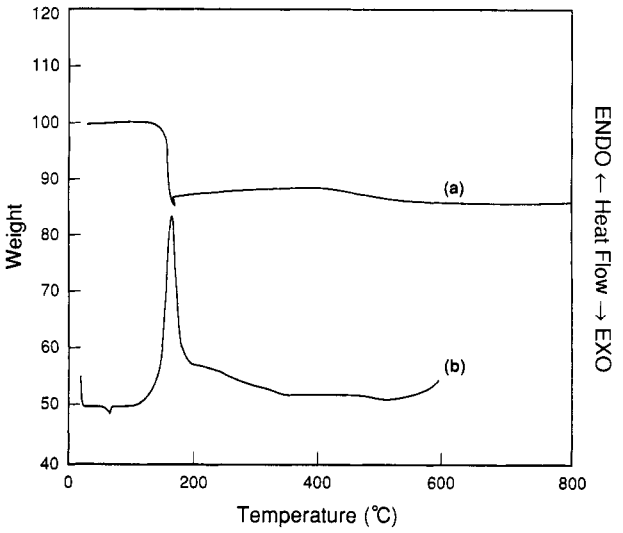

Figure 1. Thermal analyses of decaborane–dicyanopentane polymer (a) TGA, (b) DSC.

Studies of the thermolytic reactions of the polymer showed that it could be converted to BCN materials with good char yields. Thus, as shown in Figure 1a, a TGA analysis of the polymer thermal decomposition process revealed an initial weight loss occurring at 150 °C, followed by a gradual weight loss in the region of 350–500 °C. In agreement with this observation, a strong exotherm was found in the DSC trace (Figure 1b) corresponding to the first weight loss. The ceramic conversion reaction was complete at 500 °C, with a resulting 86% ceramic yield. This observed ceramic yield is higher than that calculated for the formation of only B_4C and BN (76%), but near that for loss of only hydrogen (90%), indicating that the char must contain substantial amounts of free carbon. In separate experiments, bulk pyrolysis of the polymer under an argon atmosphere at 1250 °C (1 h) and 1450 °C (12 h) afforded black materials in 78% and 64% char yields, respectively. The DRIFT spectra of both ceramics show broad absorptions near 1450 and 850 cm^{-1}, respectively, suggesting the presence of boron nitride.[12] Elemental analyses showed that the hydrogen contents of both materials were quite low (<0.05%) indicating that the polymer decomposition was complete. Assuming that the materials are composed of BN, B_4C, and C, then the analyses correspond to $(BN)_{1.0}(B_4C)_{1.1}C_{1.6}$ and $(BN)_{1.0}(B_4C)_{0.8}C_{1.3}$ compositions, respectively. As shown in Figure 2, the X-ray powder diffraction spectrum (XRD) of the 1250 °C ceramic showed only broad amorphous peaks centered near 20° and 40° 2θ. In the 1450 °C material, peaks characteristic of boron carbide and turbostratic graphite and/or boron nitride were observed.

According to the elemental analysis, upon pyrolysis to 1900 °C for 25 h, significant loss of nitrogen, presumably in the form of N_2, occurs to give a material in 49% ceramic yield with an elemental composition in agreement with a $(BN)_{1.0}(B_4C)_{4.0}C_{10.2}$ mixture. Consistent with this result, the DRIFT spectrum of the 1900 °C material showed only a weak absorption for boron nitride at 1450 cm^{-1}. Likewise, the X-ray powder diffraction spectrum of this material

(8) (a) Peshev, P.; Leyarovska, L.; Bliznakov, G. *J. Less-Common Met.* **1968**, *15*, 259–267. (b) Peshev, P.; Bliznakov, G. *J. Less-Common Met.* **1968**, *14*, 23–32.
(9) Walker, J. K. *Adv. Ceram. Mater.* **1988**, *3*, 602–604.
(10) Steinitz, R. *Modern Materials*; Hausner, H. H., Ed.; Academic Press: New York, 1960; Vol. 2, pp 191–224.
(11) See for example: (a) Mirabelli, M. G. L.; Sneddon, L. G. *J. Am. Chem. Soc.* **1988**, *110*, 3305–3307. (b) Rees, Jr., W. S.; Seyferth, D. *J. Am. Ceram. Soc.* **1988**, *71*, C194–C196. (c) Rees, Jr., W. S.; Seyferth, D. *Chem. Mater.* **1991**, *3*, 1106–1116. (d) Seyferth, D.; Rees, Jr., W. S.; Haggerty, J. S.; Lightfoot, A. *Chem. Mater.* **1989**, *1*, 45–52.
(12) Paine, R. T.; Narula, C. K. *Chem. Rev.* **1990**, *90*, 73–91.

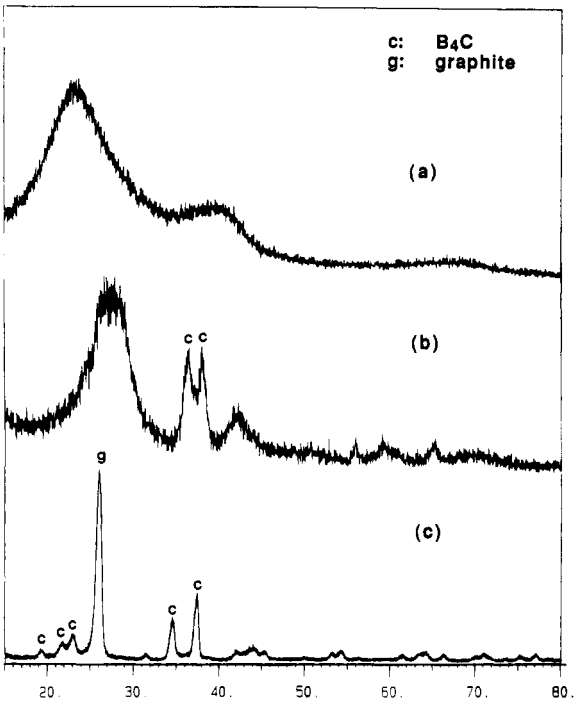

Figure 2. X-ray diffraction patterns of ceramics derived from the decaborane–dicyanopentane polymer processed at (a) 1250 °C, 1 h (b) 1450 °C, 12 h, (c) 1900 °C, 25 h.

showed boron carbide and graphite as the only crystalline phases. The crystallization of B_4C at similar temperatures has been observed in the ceramic conversion reactions of $B_{10}H_{12}$–diamine and $B_{10}H_{12}$·Ph_2POPPh_2 polymers.[11b-d]

The metal oxide/polymer dispersions were prepared by adding a metal oxide to a THF solution of the polymer, followed by vacuum evaporation of the solvent. The dispersions were obtained as slightly air-sensitive yellow solids, which were stored under argon until pyrolysis. The metal/boron/carbon ratios in the dispersions were adjusted by varying the metal oxide/polymer ratios in the mixtures. In all samples, about 25% excess of the polymer over that required for the stoichiometric formation of the diboride was used. Submicron sized metal oxides were found to give the most homogeneous mixtures.

In each case, pyrolysis of the solid metal oxide/polymer dispersion, under argon or in vacuo, produced metal diborides in excellent chemical and ceramic yields:

$$(-B_{10}H_{12}N{\equiv}C(CH_2)_5C{\equiv}N-)_n + MO_2 \text{ or } M_2O_5 \xrightarrow{\Delta} MB_2 \quad (4)$$

M = Ti, Zr, Hf, Nb, Ta

The metal oxide/polymer dispersions employing TiO_2, ZrO_2, HfO_2, Nb_2O_5, and Ta_2O_5 gave the metal diborides as the only crystalline products, as indicated by their X-ray powder diffraction spectra. The elemental analyses of Ti, Zr, Nb, and Ta boride samples prepared at ≥1450 °C exhibited near 1:2 metal:boron ratios. However, the HfO_2 dispersions were only about 60% reacted (as estimated by their XRD spectra) at this temperature and required higher temperature processing to obtain complete reaction. The O, C, and N impurities were found to depend upon the reaction temperature and time, with the nitrogen and carbon contents low at temperatures ≥1450 °C.[13] The oxygen contents decreased with elevated reaction temperatures. For example, the oxygen contents for the ZrB_2 samples prepared at 1450 (21 h), 1650 (7 h), and 2000 °C (3 h) were 4.97, 1.53, and 0.2% respectively.

The grain sizes and microstructure of the metal boride powders were found to depend upon the metal and the processing conditions. As reported in our earlier communication,[5] scanning electron microscopy (SEM) studies of the TiB_2 and ZrB_2 powder samples showed particle sizes of 2–5 μm at 2000 °C, but submicron crystallites at lower temperatures. Transmission electron microscopy (TEM) was used to investigate the morphology and microstructural development. As shown in Figure 3a,b, both the TiB_2 and ZrB_2 samples prepared at 1300 °C (2 h) contained nanometer-sized TiB_2 or ZrB_2 particles. As suggested by the higher than theoretical ceramic yields (theor for TiB_2 48.9%; obs 58.2%; theor for ZrB_2 61.1%; obs 67.6%) and the XRD results, both samples at this temperature contained either small amounts of intermediate species or unreacted oxide. The identification of the impurity phase in these samples was impossible by electron diffraction, because of the small particle sizes. When the samples were heated at 1450 °C for 1 h (Figure 3c,d), the amorphous phase between the TiB_2 and ZrB_2 grains decreased and further crystallization of the borides was observed. The samples annealed at 1450 °C for 21 h (Figures 3e,f) show significant grain growth. In agreement with these results, the XRD spectra for TiB_2 and ZrB_2 prepared at higher temperatures or longer times exhibited sharper diffraction peaks than those from samples prepared at low temperatures. In the NbB_2 and TaB_2 systems, the TEM micrographs of the 1300 °C materials (2.5 h) showed larger grains (0.5–1.0 μm) than the TiB_2 and ZrB_2 samples (50–100 nm) annealed at the same temperature. The NbB_2 and TaB_2 samples prepared at 1480 °C had an average grain size of 1.0 μm, as estimated by TEM. Only slight grain growth was found for the 1900 °C samples.

The ceramic conversion processes for the metal oxide/polymer dispersions were followed by the TGA-DTA-MS method. As shown in Figure 4, three weight losses were observed for all metal oxide dispersions. An initial two-step weight loss (8–15%), consistent with the evaporation of residual THF solvent and polymer decomposition, occurred in the 50–580 °C range for each sample and was found to be independent of the oxide identity. Mass spectral analyses of the volatile decomposition products showed predominantly THF during the first weight loss (50–180 °C) and methane in the second (300–580 °C). A strong exotherm was observed in the DTA at the end of the first weight loss, suggesting that the decomposition of the polymer also occurred at this temperature. No significant weight change was found in the 580–1250 °C region. The major weight losses for all samples took place at temperatures higher than 1250 °C, corresponding to the subsequent reduction of the metal oxides to metal borides.

The XRD analyses of the TiO_2, Nb_2O_5, and Ta_2O_5 polymer dispersions pyrolyzed at 580 °C showed only peaks corresponding to metal oxides, suggesting an initial polymer decomposition to amorphous BCN materials.

(13) Since low carbon (0.16%) was observed in all other materials prepared at temperatures below 1650 °C, the increased carbon in the NbB_2 (0.80%) and TaB_2 (2.69%) samples at 1900 °C may have resulted from contamination by the carbon crucibles.

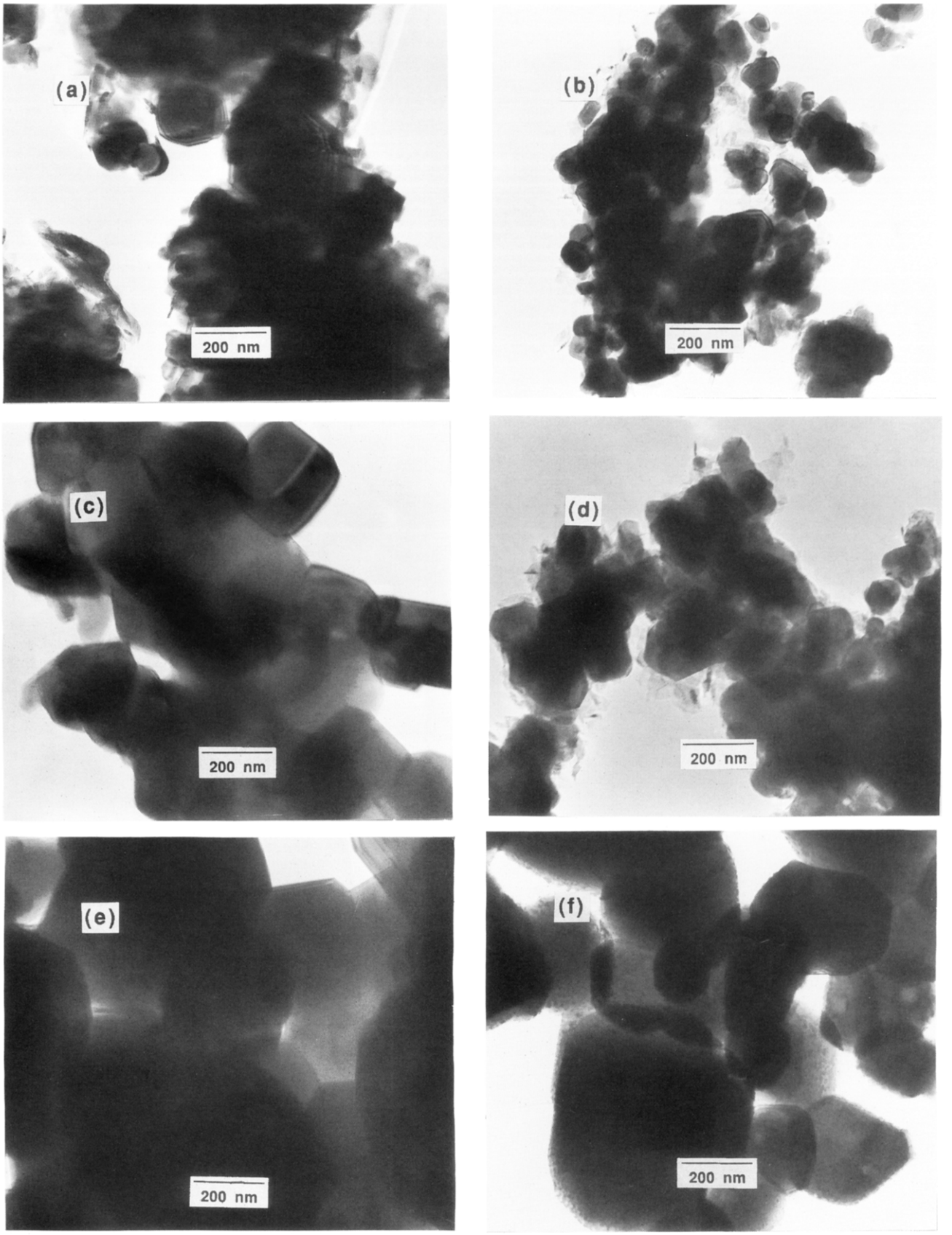

Figure 3. TEM micrographs of (a) TiB_2, 1300 °C, (b) ZrB_2, 1300 °C, (c) TiB_2, 1450 °C, 1 h, (d) ZrB_2, 1450 °C, 1 h, (e) TiB_2, 1450 °C, 21 h, (f) ZrB_2, 1450 °C, 21 h.

Consistent with these results and the polymer decomposition studies discussed earlier, the DRIFT spectra of these materials showed no BH stretching absorptions. A typical TEM micrograph for the TiO_2 material (580 °C) is given in Figure 5, which shows submicron TiO_2 particles embedded in an amorphous BNC matrix.

The subsequent reduction of the metal oxides to metal diborides was found to proceed differently depending upon the metal. The experimental data for the TiO_2/polymer system suggest that, following initial polymer decompo-

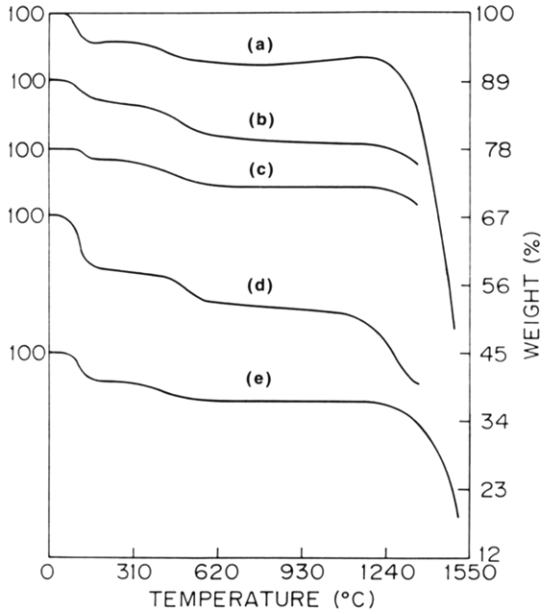

Figure 4. TGA analyses of metal oxide/polymer dispersions: (a) TiO_2, (b) ZrO_2, (c) HfO_2, (d) Nb_2O_5, (e) Ta_2O_5.

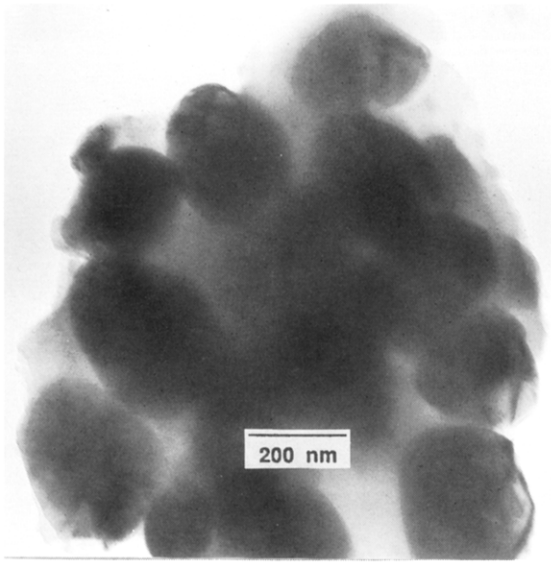

Figure 5. TEM micrograph of TiO_2/polymer dispersions pyrolyzed at 580 °C for 2 h.

$$TiO_2/\text{polymer} \rightarrow TiO_2/\text{“BCN”} + H_2 \quad (5)$$

$$3TiO_2 + 3B + 2C \rightarrow TiBO_3 + 2TiC + B_2O_3 \quad (6)$$

$$3TiO_2 + 10B \rightarrow 3TiB_2 + 2B_2O_3 \quad (7)$$

$$TiO_2 + 3C \rightarrow TiC + 2CO \quad (8)$$

$$2TiBO_3 + 5C \rightarrow 2TiC + B_2O_3 + 3CO \quad (9)$$

$$TiC + B_2O_3 + 2C \rightarrow TiB_2 + 3CO \quad (10)$$

sition (eq 5), titanium borate, titanium carbide and boron oxide form in the reaction of TiO_2 with the BCN material by one or more of the reactions shown in eqs 6–8. At higher temperatures further reaction (eqs 9 and 10) to produce the final titanium diboride product occurs.

Thus, as shown in Figure 6b, when the TiO_2 dispersion was heated at 1000 °C for 2 h, the TiO_2 completely

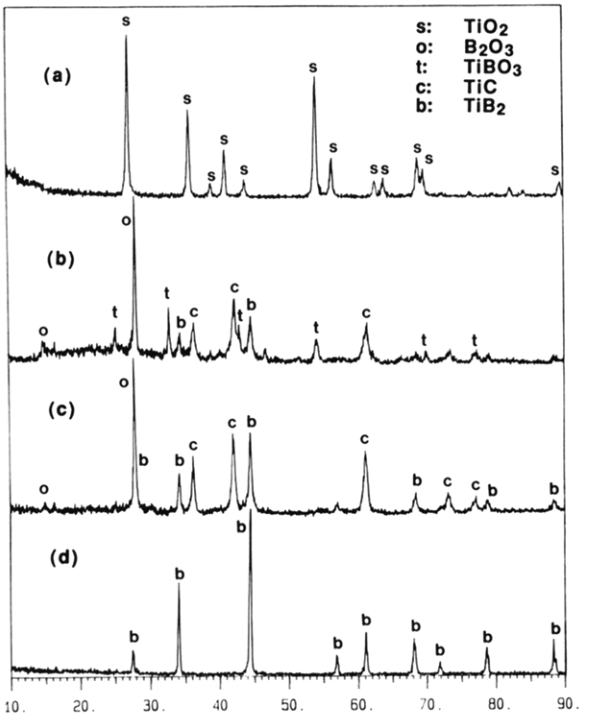

Figure 6. X-ray diffraction patterns of TiO_2/polymer dispersions heated for 2 h at (a) 580 °C, (b) 1000 °C, (c) 1100 °C, (d) 1450 °C.

disappeared and the material was found to be composed of $TiBO_3$, TiC, B_2O_3, and a small amount of TiB_2. The X-ray pattern of B_2O_3 is similar to that of H_3BO_3, but the absence of an O–H stretching absorption in the DRIFT spectrum of the 1000 °C material is consistent with the presence of only B_2O_3. The formation of TiB_2 at temperatures near 1000 °C by borothermal reduction (eq 7) has also been observed in other systems.[8b,9,14,15] Similarly, the formation of TiC and boron oxide as reaction intermediates was found by Rhine[15] in the thermal decomposition of $B/((FuO)_{0.63}(BuO)_{0.37}TiO_{1.5})_n$ (FuOH = furfuryl alcohol).

The XRD pattern (Figure 6c) of the material annealed at 1100 °C showed only diffraction peaks corresponding to TiC, TiB_2, and B_2O_3. The complete disappearance of $TiBO_3$ indicates that the borate is formed at the initial stage of the reaction and that its further reaction (eq 9) with the amorphous carbon present in the material results in TiC and B_2O_3. The TEM micrograph (Figure 7) showed that the 1100 °C material was composed of nanometer-sized crystals, along with the amorphous phase. Since no weight loss occurred over the 580–1250 °C range, the loss of nitrogen (as N_2, NO, etc.) does not seem likely. Although the formation of crystalline TiN by carbothermal reduction of TiO_2 under nitrogen at 1100 °C has been reported,[16] no evidence of crystalline metal nitride or carbonitride was found in the XRD spectra of the TiO_2/polymer dispersions pyrolyzed above 1100 °C. Therefore, the nitrogen must be present in the amorphous phase, presumably, as boron

(14) Barton, L.; Nicholls, D. *J. Inorg. Nucl. Chem.* **1966**, *28*, 1367–1372.
(15) Jiang, Z.; Rhine, W. E. *Chem. Mater.* **1992**, *4*, 497–500.
(16) (a) White, G. V.; Mackenzie, K. J. D.; Johnston, J. H. *J. Mater. Sci.* **1992**, *27*, 4287–4293. (b) White, G. V.; Mackenzie, K. J. D.; Brown, W. M.; Bowden, M. E.; Johnston, J. H. *J. Mater. Sci.* **1992**, *27*, 4294–4299.

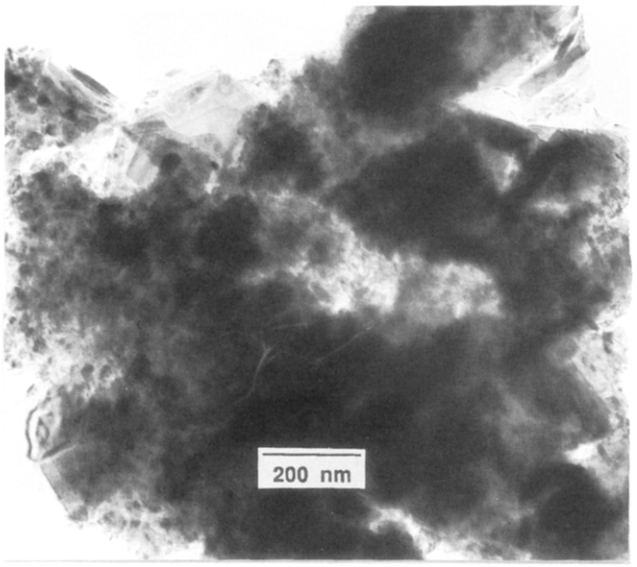

Figure 7. TEM micrograph of a TiO_2/polymer dispersion pyrolyzed at 1100 °C for 2 h.

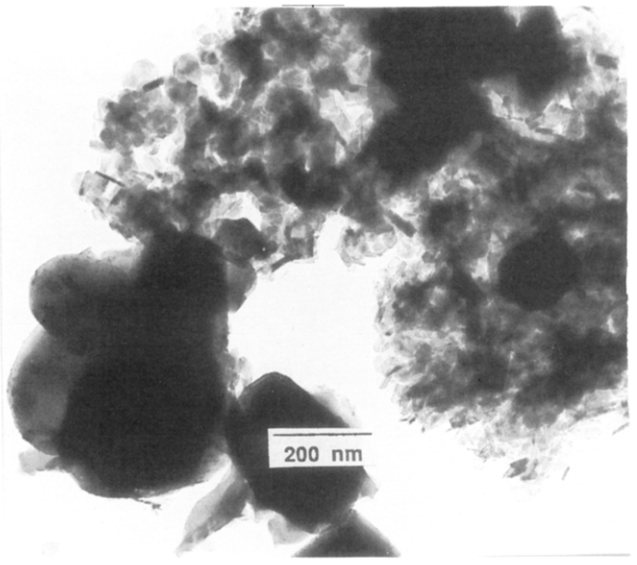

Figure 8. TEM micrograph of TiB_2 sample prepared at 1450 °C for 1 h.

nitride. The absence of TiN is not surprising, since it is unstable in the presence of boron at ≥1100 °C.[17] At 1300 °C, TiB_2 was formed as the major crystalline phase. The reduction of TiO_2 was complete when the sample was annealed at 1450 °C for 1 h (Figure 6d). Although the XRD spectrum for this material showed TiB_2 as the only crystalline phase, the TEM micrograph exhibited evidence of small amounts of residual materials, presumably boron oxide, with the typical appearance shown in Figure 8. No such materials were observed when the sample was heated for a longer time (1450 °C, 21 h) or at a higher temperature (1900 °C, 3 h).

In the Nb_2O_5/ and Ta_2O_5/polymer systems, the X-ray diffraction patterns of the ceramics prepared at different temperatures suggest the reaction sequence, shown in eqs 11–15, for the reduction of the metal oxides. These reactions involve the initial formation of metal carbide, B_2O_3 and/or metal monoborides (eqs 12 and 13), followed

(17) Matsudaira, T.; Itoh, H.; Naka, S.; Hamamoto, H.; Obayashi, M. *J. Mater. Sci.* **1988**, *23*, 288–292.

$$M_2O_5/\text{polymer} \rightarrow M_2O_5/\text{“BCN”} \quad (11)$$

$$M_2O_5 + 7C \rightarrow 2MC + 5CO \quad (12)$$

$$3M_2O_5 + 19B \rightarrow 3MB + 3MB_2 + 5B_2O_3 \quad (13)$$

$$4MC + 3B_2O_3 + 5C \rightarrow 2MB_2 + 2MB + 9CO \quad (14)$$

$$MB + B \rightarrow MB_2 \quad (15)$$

$$M = \text{Nb or Ta}$$

by the conversion of these species to the diborides at higher temperatures (eqs 14 and 15).

Thus, as shown in the XRD patterns in Figure 9b, NbC and B_2O_3 were formed as the only crystalline phases in the sample pyrolyzed at 1100 °C for 2.5 h. The onset of NbB_2 crystallization was found at 1200 °C (Figure 9c). NbB was also observed as a minor product at this temperature. Upon treatment at 1300 °C for 2.5 h, NbC completely disappeared and the material was composed of NbB_2 with a small amount of NbB. The NbB_2 was the only product in the 1480 °C sample (Figure 9d). A similar reaction sequence was also observed by XRD in the Ta_2O_5/polymer system, except that TaB was formed as a major product in the material annealed at 1200 °C (Figure 10c). The monoboride was completely converted to the diboride when the sample was treated at 1300 °C for 2.5 h (Figure 10d).

In contrast to the above observations, no intermediate species were observed in the ZrO_2 and HfO_2/polymer systems. The XRD patterns of the materials obtained before completion of the reactions showed only the unreacted metal oxides and the diborides. For example, as shown in Figure 11a, no reaction was observed between the ZrO_2 and the BCN material at 1000 °C, but the 1450 °C material contained ~90% crystalline ZrB_2, together with unreacted ZrO_2 (Figure 11b). The reaction was complete when the sample was pyrolyzed at 1450 °C for 21 h (Figure 11c). Similar results were observed in the HfO_2/polymer system (Figure 12), except that a higher reaction temperature (1900 °C) was necessary to drive the reaction to completion. These observations suggest that ZrO_2 and HfO_2 react with the BCN material in one step, as shown in eq 16 or that alternately the initial formation of carbides and boron oxide is followed by a fast reaction to produce the borides (eqs 17 and 18).

$$MO_2 + 2B + 2C \rightarrow MB_2 + 2CO \quad (16)$$

or

$$3MO_2 + 3C + 4B \rightarrow 3MC + 2B_2O_3 \quad (17)$$

$$MC + B_2O_3 + 2C \xrightarrow{\text{fast}} MB_2 + 3CO \quad (18)$$

$$M = \text{Zr or Hf}$$

The latter explanation would imply that the ZrC and HfC are much more reactive than TiC and react with boron oxide to give diborides immediately after their formation.

TiB_2 Coatings on Graphite Plates. Metal boride coatings have been used in a number of important practical applications. For example, TiB_2 has been used as a coating

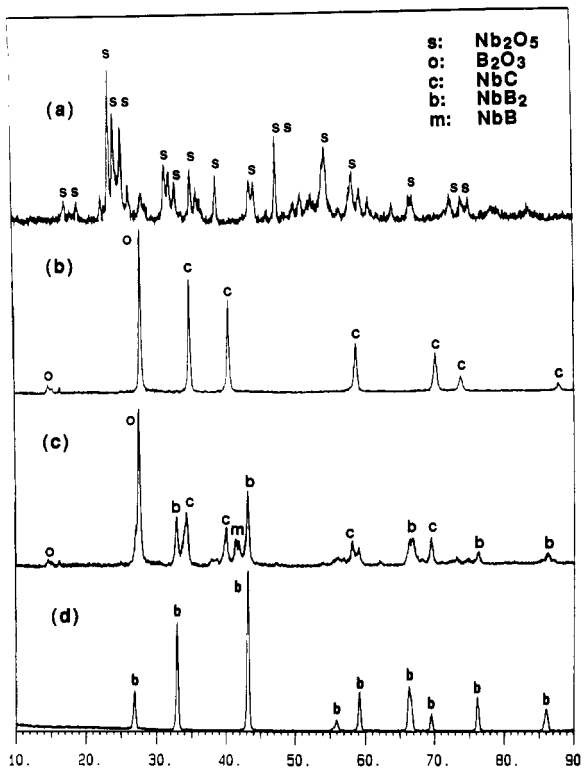

Figure 9. X-ray diffraction patterns of Nb_2O_5/polymer dispersions heated for 2.5 h at (a) 580 °C, (b) 1100 °C, (c) 1200 °C, (d) 1480 °C.

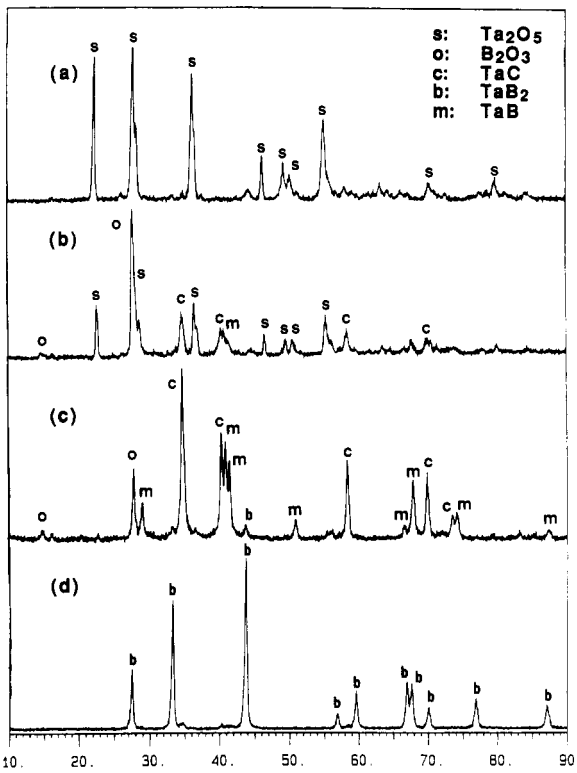

Figure 10. X-ray diffraction patterns of Ta_2O_5/polymer dispersions heated for 2.5 h at (a) 580 °C, (b) 1100 °C, (c) 1200 °C, (c) 1300 °C.

material for the protection of electrodes from chemical corrosion and for a hard coating on tools.[1b] There have been a number of reports on the generation of titanium and zirconium diboride films by chemical vapor deposition (CVD)[3] or physical vapor deposition (PVD)[4] methods. A solution method of achieving such coatings would clearly

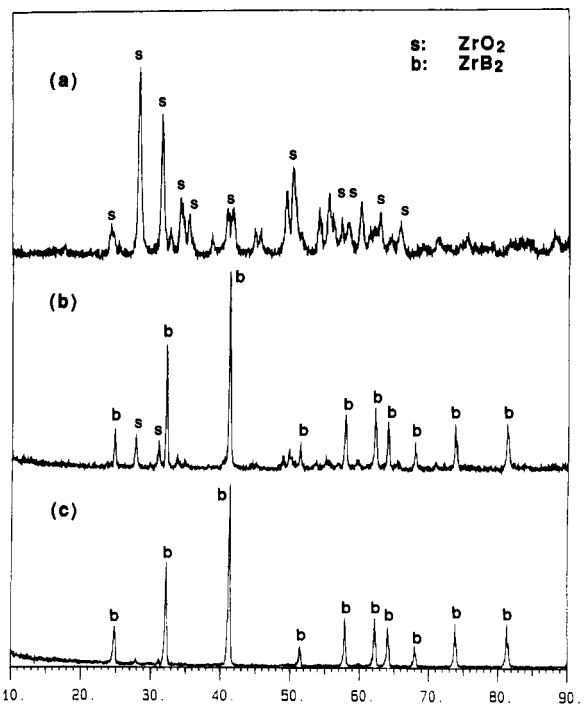

Figure 11. X-ray diffraction patterns of ZrO_2/polymer dispersions heated for 2.5 h at (a) 1000 °C, (b) 1450 °C, (c) 1480 °C.

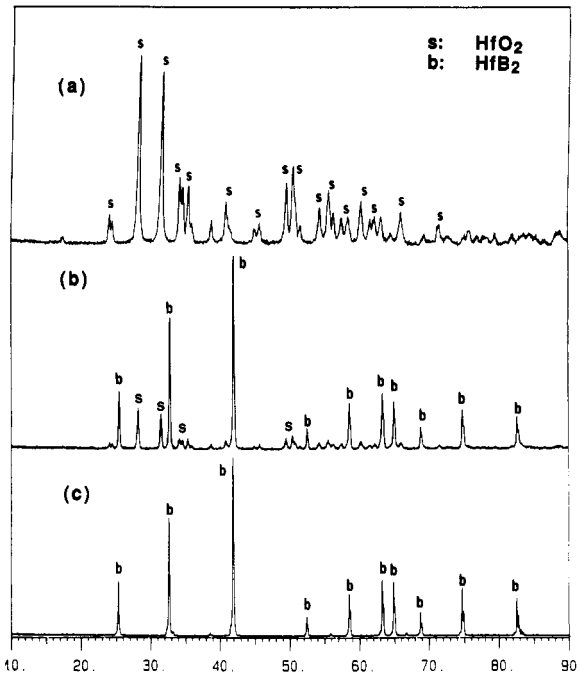

Figure 12. X-ray diffraction patterns of (a) HfO_2, (b) HfO_2/polymer dispersion heated at 1450 °C (2.5 h), and (c) HfO_2/polymer dispersion heated at 1900 °C (2.5 h).

have a number of advantages; therefore, the use of the polymer/metal oxide systems described above for the formation of metal boride coatings on graphite surfaces was explored.

To obtain a homogeneous dispersion, an organic polymeric surfactant, du Pont AB dispersant, was used in the system to enhance the suspension. The major requirements for the surfactant in this system are that it stabilizes the TiO_2 particles over a moderate temperature range and contribute no additional impurities. Since, as shown in the Experimental Section, the surfactant decomposes at temperatures well below the reduction temperature of TiO_2

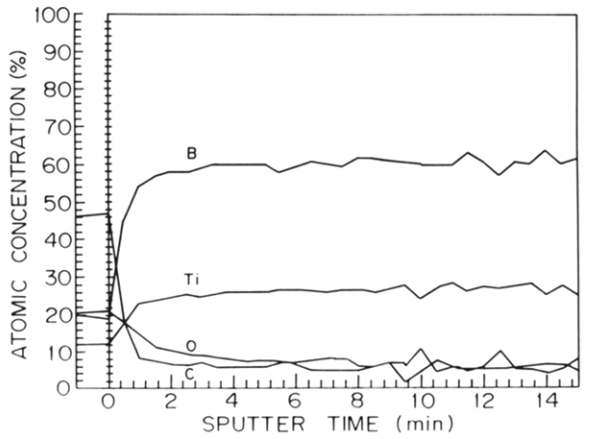

Figure 13. Auger depth profile of a TiB_2 coating on a graphite plate.

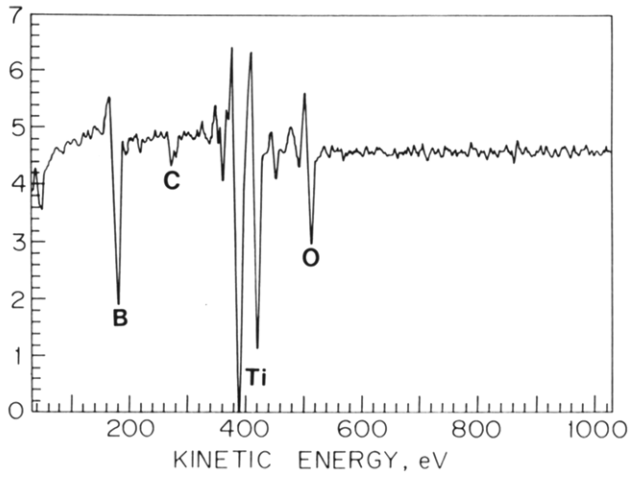

Figure 14. Auger spectrum of a TiB_2 coating on a graphite plate after sputtering for 15 min.

to give only trace residues, the formation of titanium diboride should not be affected by the addition of this surfactant.

In a typical process, a suspension of TiO_2 in THF was prepared by complete mixing of submicron TiO_2 powder, decaborane–dicyanopentane polymer and dispersant by means of ultrasonic agitation. The emulsion thus formed remained suspended for only a short period of time (<0.5 h) and had to be used immediately. The precursor coatings were obtained by either dipping the substrate into the emulsion or by dispersing the emulsion on the carbon plates. The thickness of TiB_2 dispersion was adjusted by either multiple coatings or by increasing the viscosity of the precursor solution. Subsequent pyrolysis of the coated carbon plates under argon or in vacuo above 1450 °C produced TiB_2 coatings.

An Auger analysis of the elemental composition of the coating annealed at 2000 °C showed a nearly 1:2 titanium:boron ratio. As can be seen in the sputter depth profile (Figure 13), the Ti/B ratio becomes constant after sputtering through ~250 Å (2 min). The C and O levels are low and constant throughout the thickness of the coating. The major peaks in the spectrum taken after sputtering for 15 min (Figure 14) correspond to Ti and B, in addition to a small amount of carbon and oxygen. The X-ray diffraction pattern of a coated surface annealed at 2000 °C (Figure 15) shows crystalline TiB_2, in addition to the diffraction peaks arising from the graphite substrate.

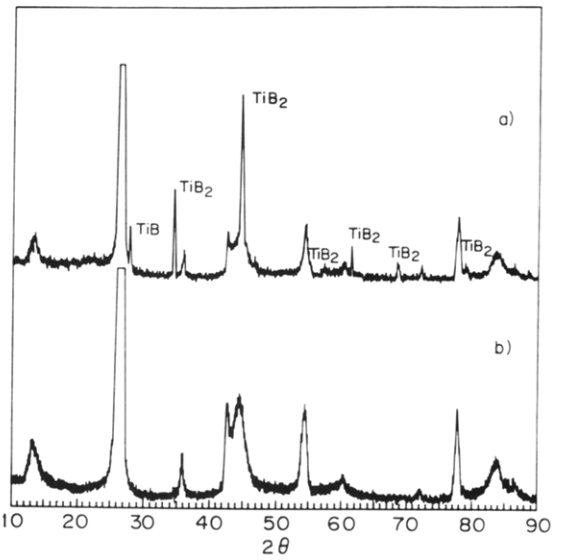

Figure 15. X-ray diffraction patterns of (a) a TiB_2 coating on a graphite plate and (b) an uncoated graphite plate.

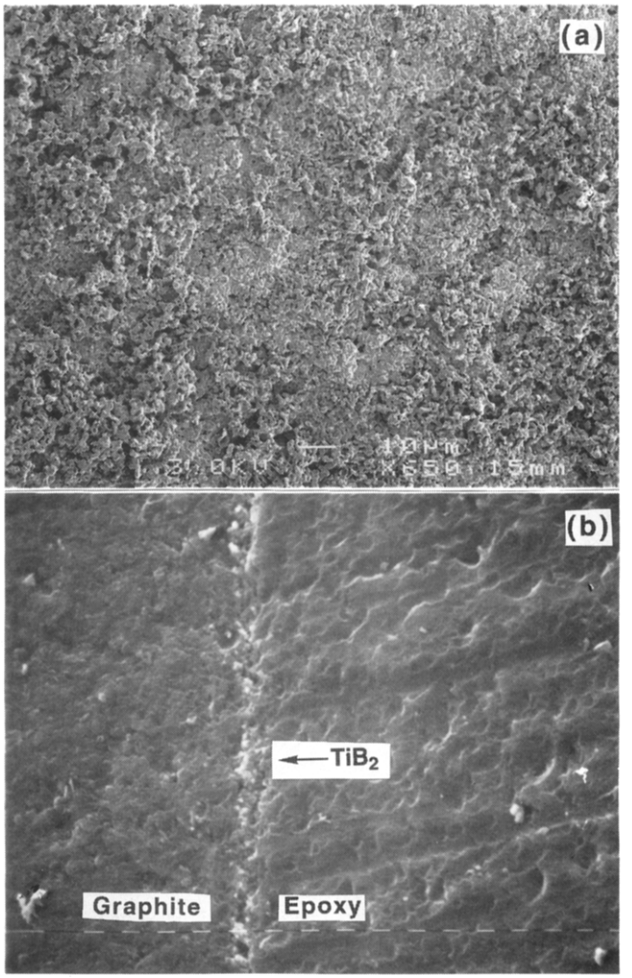

Figure 16. Scanning electron micrograph (SEM) of a TiB_2 coating on a graphite plate (a) surface and (b) cross section.

Consistent with bulk pyrolysis results, no other crystalline species were observed.

The scanning electron micrograph (SEM) of a coated graphite plate pyrolyzed at 1450 °C for 2 h (Figure 16) shows that a homogeneous, porous TiB_2 coating is formed on the surface. Consistent with the bulk pyrolysis results, the coatings prepared at 1450 °C were composed of crystalline TiB_2. When the coatings were heated

at 2000 °C, larger crystals (2–4 μm) were formed. Due to the grain coarsening, the coatings prepared at high temperatures are more porous than those made at low temperatures. These preliminary results on TiB_2 coatings suggest that polymer/submicron metal oxide dispersions along with a suitable surfactant should be useful for the generation of a variety of metal boride coatings of potential technological importance.

In conclusion, we have demonstrated that metal boride powders in good purity can be prepared by the solid-state reduction of metal oxide/polymer dispersions. In the Ti, Zr, Hf, Nb, Ta systems, the metal diborides are formed as the only crystalline products, with the grain sizes depending on the processing conditions. The reaction pathways leading to the formation of diborides are found to be metal dependent. Because of the processability of the polymer, the liquid TiO_2/polymer dispersion containing a suitable surfactant can be used to generate TiB_2 coatings on graphite substrates.

Acknowledgment. We thank the Department of Energy, Division of Chemical Sciences, Office of Basic Energy Sciences for the support of this work. Additional support and facilities were also provided by the National Sciences Foundation—Materials Research Laboratory at the University of Pennsylvania. We also thank Dr. Michael Fyrd (du Pont) for the samples of submicron metal oxides and the surfactant, Dr. Joe Barendt (Callery) for a gift of decaborane(14), Dr. Andrew R. McGhie for the TGA/DTA results, Mr. J. Bruce Rothman for the Auger results, Ms. Xueqin Wang for assistance in obtaining the TEM and SEM photographs and Mr. William Romanow for help in the use of the Astro furnace.